Article:
Tangsombun, Chayanan, Simpson, Amy Melissa, Genever, Paul et al. (2025) Diffusion-Patterned Multi-Component Supramolecular Gels Loaded with Gold Nanoparticles Direct Mesenchymal Stem Cell Growth and Differentiation. Advanced Healthcare Materials. 2405057. ISSN: 2192-2659

https://doi.org/10.1002/adhm.202405057

Supporting Information

Diffusion-Patterned Multi-Component Supramolecular Gels Loaded with Gold Nanoparticles Direct Stem Cell Growth and Differentiation

*Chayanan Tangsombun[1], Amy Simpson[2], Paul G. Genever[2] and David K. Smith[1]**

[1]Department of Chemistry, University of York, Heslington, York, YO10 5DD, UK
[2]Department of Biology, University of York, Heslington, York, YO10 5DD, UK

SUPPLEMENTARY INFORMATION

S1 $AuCl_3$ uptake
S2 Transmission Electron Microscopy (TEM)
S3 Thermal Stability
S4 Rheology
S5 AuNP patterning
S6 Biology Studies

S1 $AuCl_3$ uptake

Table S1. Rate of Au(III) uptake in hydrogels over time as determined by UV-Vis spectroscopy.

TIME (hours)	AVERAGE %Au(III) uptake				
	DBS-$CONHNH_2$ (0.3% wt/vol)	DBS-$CONHNH_2$/GG (0.3% wt/vol DBS-$CONHNH_2$ and 0.5% wt/vol GG)	DBS-$CONHNH_2$/GG (0.3% wt/vol DBS-$CONHNH_2$ and 1.0 % wt/vol GG)	GG (0.8% wt/vol)	GG (1.3% wt/vol)
1	75.8	29.3	35.6	28.7	26.2
3	83.8	61.5	55.5	32.4	29.5
5	86.0	73.8	65.0	30.2	34.0
24	100.0	100.0	100.0	31.5	35.0

Table S2. Maximum amount of Au (III) loaded into each hydrogel in terms of μmoles and percentage.

Gel	DBS-$CONHNH_2$ Loading	Gellan Gum Loading	Total Loading	μmoles Au /mL gel	% Au uptake	Standard error of % Au uptake
DBS-$CONHNH_2$	0.3%	-	0.3%	17.3	86.6	0.86
Hybrid	0.3%	0.5%	0.8%	15.5	77.6	0.71
Hybrid	0.3%	1.0%	1.3%	15.5	77.6	0.41
Gellan gum	-	0.8%	0.8%	9.3	46.5	0.88
Gellan gum	-	1.3%	1.3%	8.4	42.1	0.47

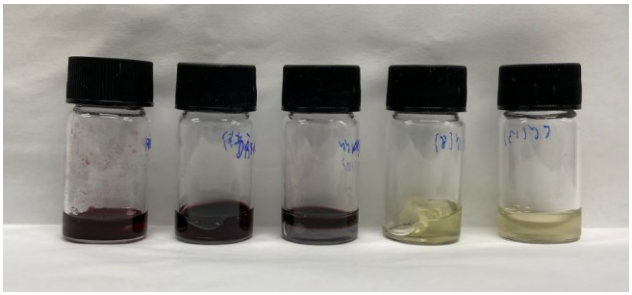

Figure S1. Photograph of gels loaded with $AuCl_3$. DBS-$CONHNH_2$ (0.3% wt/vol), DBS-$CONHNH_2$/GG (0.3% wt/vol DBS-$CONHNH_2$ and 0.5% wt/vol GG), DBS-$CONHNH_2$/GG (0.3% wt/vol DBS-$CONHNH_2$ and 1.0% wt/vol GG), and GG (0.8% wt/vol) and GG (1.3% wt/vol) from left to right.

S2 Transmission Electron Microscopy (TEM)

Gels were prepared as described in Section 4.2 of the paper and an $AuCl_3$ solution (1 mL, 10 mM) was added on top of each gel. After 24 h, the supernatant was removed, and the gels were washed with water (5 mL) seven times every 10-15 min. Samples for TEM were obtained by adding a small amount of each sample onto a copper grid as thinly as possible, since the two-component system was a stiff gel. Excess

sample was removed with filter paper and allowed to set for 5 minutes. A negative stain (1% uranyl acetate) was then added. Before the images were taken, the samples were left to rest for 30 minutes.

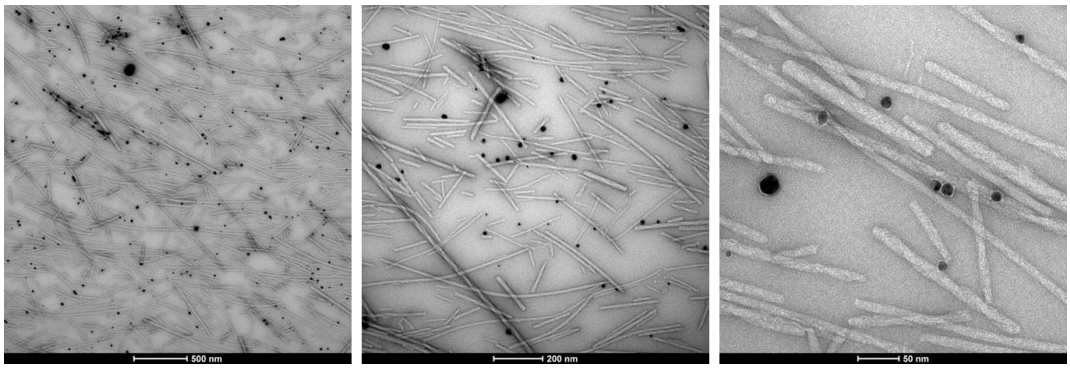

Figure S2. TEM images of DBS-$CONHNH_2$ (0.3% wt/vol) incorporating AuNPs. Scale bar: 500, 200 and 50 nm (from left to right).

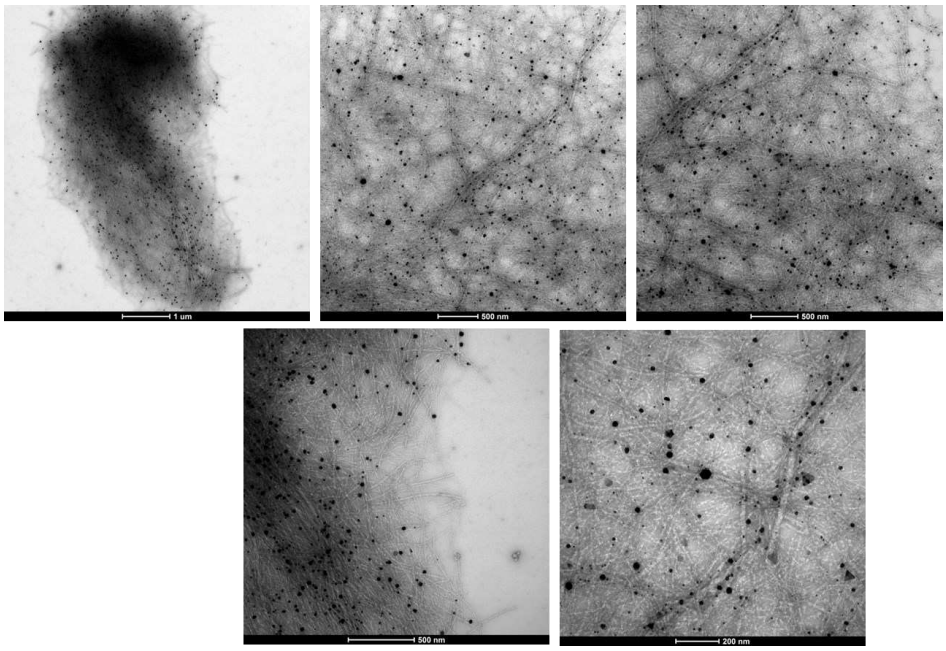

Figure S3. TEM images of DBS-$CONHNH_2$/GG (0.3% wt/vol of LMWG and 0.5% wt/vol of GG) incorporating AuNPs. Scale bar: 1 μm, 500 and 500 nm (from top left to top right). Scale bar: 500 and 20 nm (from bottom left to right).

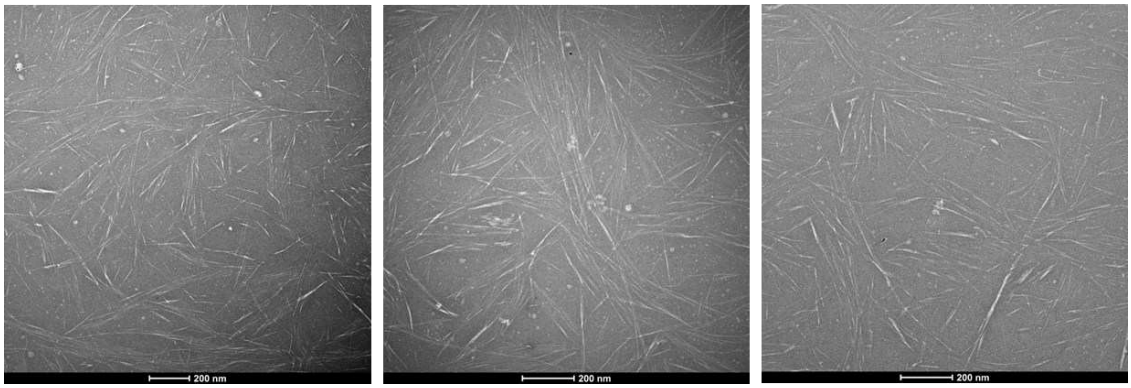

Figure S4. TEM images of gellan gum (0.8% wt/vol) loaded with $AuCl_3$. Scale bar: 200 nm.

S3 Thermal Stability Studies

All the gels were prepared as described in Section 4.2 of the paper in 7 ml vials (diameter = 2 cm, height = 6 cm). An $AuCl_3$ solution (1 mL, 5 mM) was added on top of each gel. After 24 h, the supernatant was removed, and the gels were washed with water five times. All the gels were then placed in a high precision thermoregulated oil bath with an initial temperature of 25 °C. The temperature was increased by 1 °C/min until 100 °C. The integrity of the gels was checked by tube inversion every minute. The temperature (T_{gel}) was recorded when the gel began to run down the side of the vial. These experiments were performed in triplicate and the average T_{gel} is recorded.

Table S3. T_{gel} values of gels formed by individual gelators, and DBS-$CONHNH_2$/GG hybrid gels (N = 3, mean reported). DBS-$CONHNH_2$ hydrogels was triggered by heat-cool cycle and gellan gum was cross-linked using $CaCl_2$ (5 %wt/vol) in all cases.

Gel	DBS-$CONHNH_2$ Loading	Gellan Gum Loading	Total Loading	$AuCl_3$ Loading (1 mL) added	T_{gel} (° C)
DBS-$CONHNH_2$	0.3%	-	0.3%	-	88
DBS-$CONHNH_2$	0.3%	-	0.3%	5 mM	75
Gellan Gum	-	0.8%	0.8%	-	>100
Gellan Gum	-	0.8%	0.8%	5 mM	>100
Gellan Gum	-	1.3%	1.3%	-	>100
Gellan Gum	-	1.3%	1.3%	5 mM	>100
Hybrid	0.3%	0.5%	0.8%	-	>100
Hybrid	0.3%	0.5%	0.8%	5 mM	>100
Hybrid	0.3%	1.0%	1.3%	-	>100
Hybrid	0.3%	1.0%	1.3%	5 mM	>100

S4 Rheology

Gels were prepared as described in Section 4.2 of the paper. For comparison, gels (1 mL total) were also submerged in the $AuCl_3$ solution (5 mM, 1 mL) for 24 h. The gels were transferred and placed on the rheometer using a spatula. Measurements were carried out at 25 °C using a 20 mm parallel plate and a gap of 2.5 mm. The amplitude sweep was performed in the range of 0.01-100% strain at a 1 Hz frequency. The frequency sweep was performed between 0.1-100 Hz using a shear strain of 0.15%. For reproducibility, the experiments were performed in triplicate, and average data were used to plot the graphs.

Table S4. Rheology data for gels loaded with Au and without Au.

Gel	DBS-CONHNH$_2$ Loading	Gellan Gum Loading	Total Loading	$AuCl_3$ Loading (1 mL) added	G' (Pa)	G" (Pa)	G'/G" Crossover
DBS-CONHNH$_2$	0.3%	-	0.3%	-	1050	75	5.2%
DBS-CONHNH$_2$	0.3%	-	0.3%	5 mM	485	40	6.3%
Gellan Gum	-	0.8%	0.8%	-	5440	1310	0.7%
Gellan Gum	-	0.8%	0.8%	5 mM	6365	1015	0.6%
Gellan Gum	-	1.3%	1.3%	-	15420	2060	0.6%
Gellan Gum	-	1.3%	1.3%	5 mM	19760	1455	0.5%
Hybrid	0.3%	0.5%	0.8%	-	22500	2810	1.3%
Hybrid	0.3%	0.5%	0.8%	5 mM	22020	1920	1.3%
Hybrid	0.3%	1.0%	1.3%	-	55185	5350	1.4%
Hybrid	0.3%	1.0%	1.3%	5 mM	52500	3630	1.4%

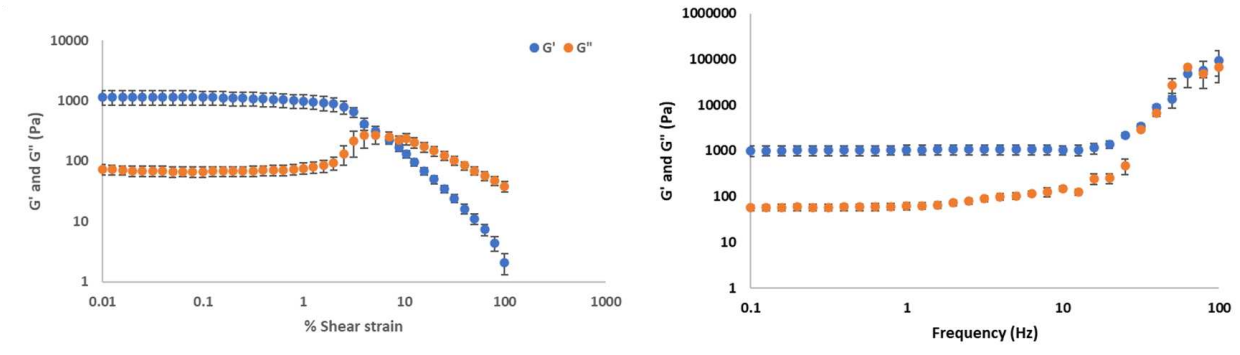

Figure S5. Elastic (G′, blue circles) and viscous (G′′, orange circles) moduli of DBS-CONHNH$_2$ hydrogel (0.3% wt/vol) with increasing shear strain (left) and frequency (right).

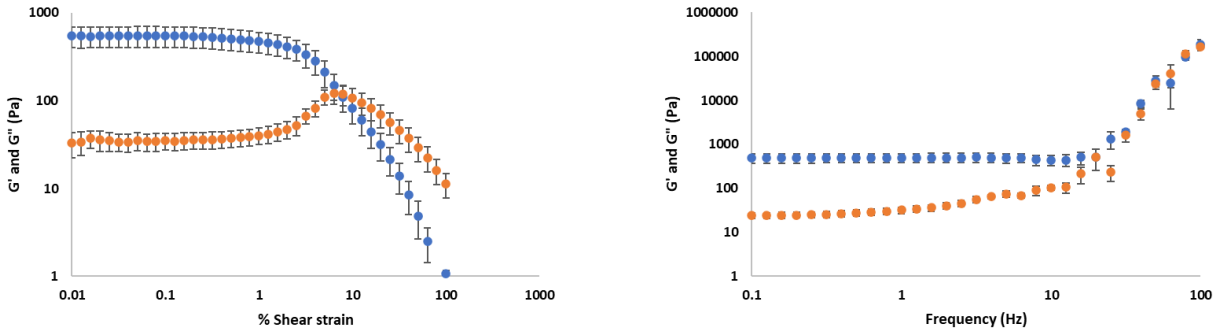

Figure S6. Elastic (G′, blue circles) and viscous (G″, orange circles) moduli of DBS-CONHNH$_2$ hydrogel (0.3% wt/vol–loaded with $AuCl_3$) with increasing shear strain (left) and frequency (right).

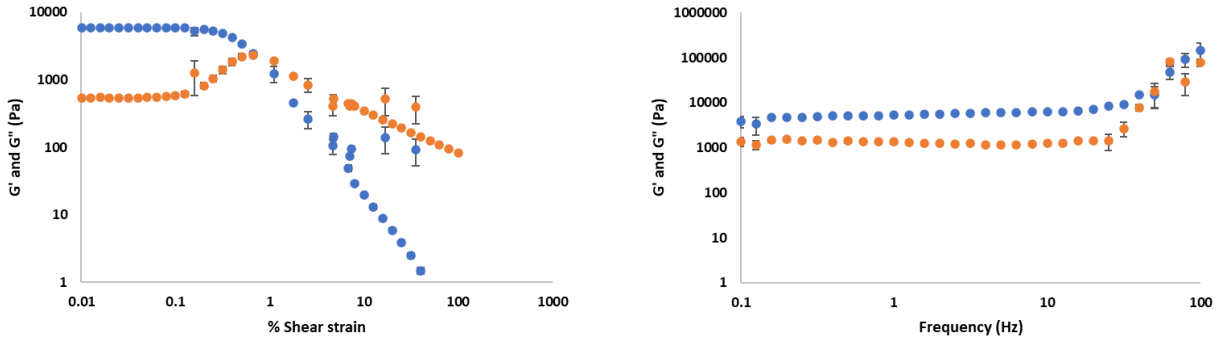

Figure S7. Elastic (G′, blue circles) and viscous (G″, orange circles) moduli of gellan gum hydrogel (0.8 % wt/vol) with increasing shear strain (left) and frequency (right).

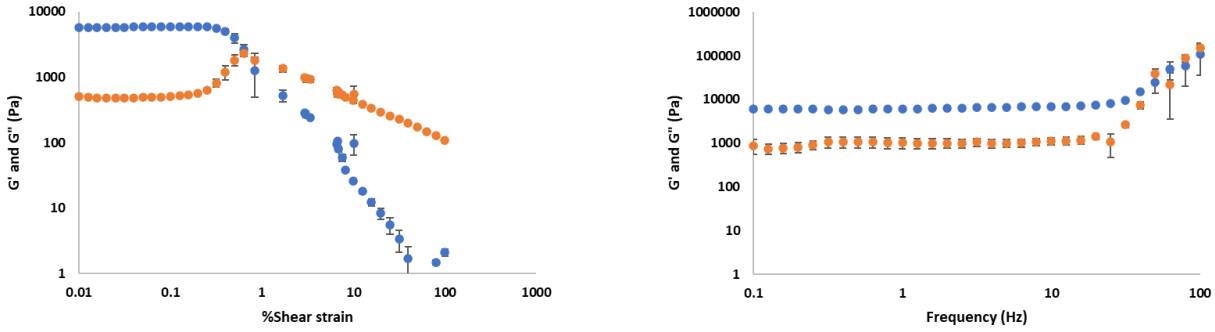

Figure S8. Elastic (G′, blue circles) and viscous (G″, orange circles) moduli of gellan gum hydrogel (0.8% wt/vol–loaded with $AuCl_3$) with increasing shear strain (left) and frequency (right).

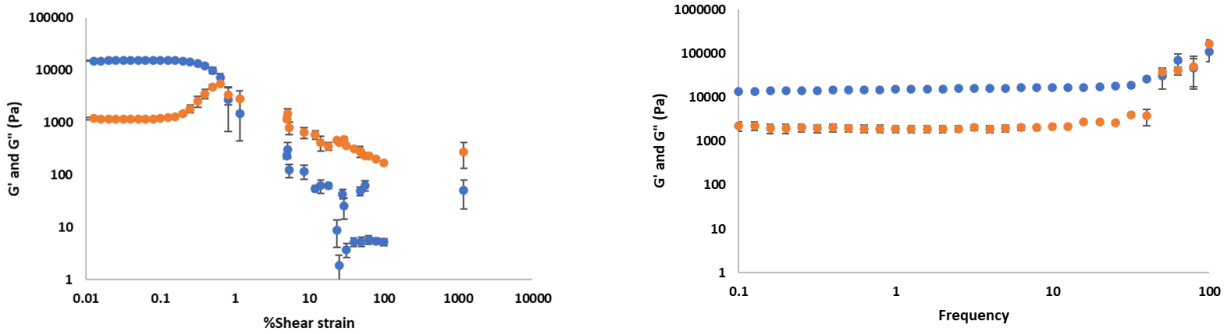

Figure S9. Elastic (G′, blue circles) and viscous (G′′, orange circles) moduli of gellan gum hydrogel (1.3 % wt/vol) with increasing shear strain (left) and frequency (right).

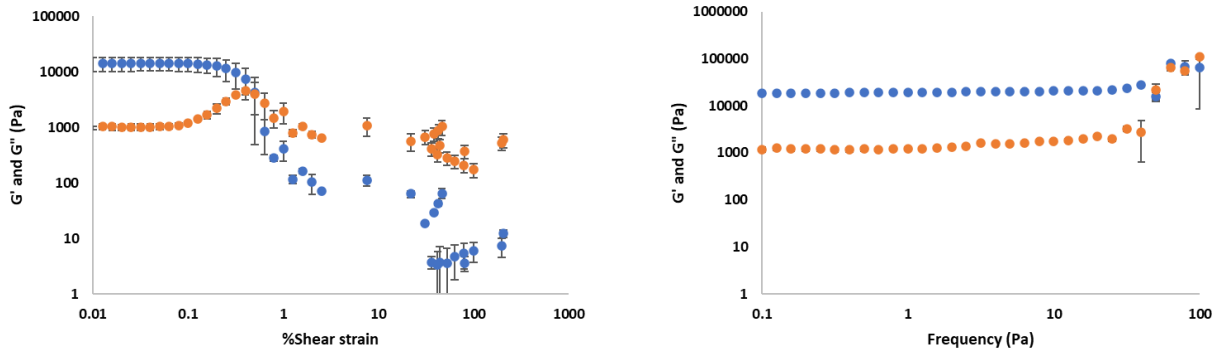

Figure S10. Elastic (G′, blue circles) and viscous (G′′, orange circles) moduli of gellan gum hydrogel (1.3 % wt/vol –loaded with $AuCl_3$) with increasing shear strain (left) and frequency (right).

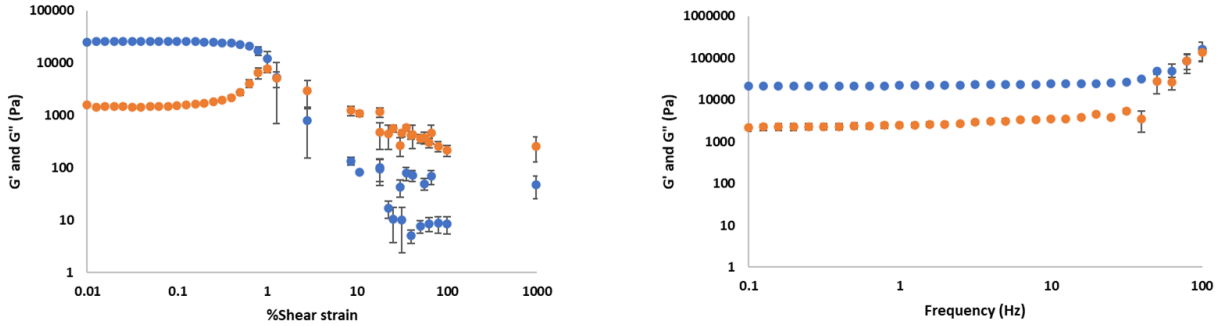

Figure S11. Elastic (G′, blue circles) and viscous (G′′, orange circles) moduli of DBS-$CONHNH_2$/gellan gum hydrogel (0.3% wt/vol DBS-$CONHNH_2$ and 0.5% wt/vol gellan gum) with increasing shear strain (left) and frequency (right).

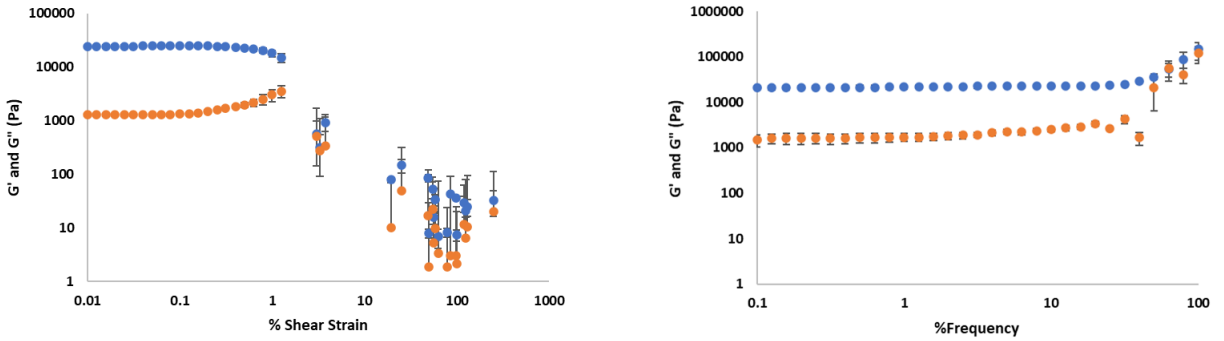

Figure S12. Elastic (G′, blue circles) and viscous (G′′, orange circles) moduli of DBS-CONHNH$_2$/gellan gum hydrogel (0.3% wt/vol DBS-CONHNH$_2$ and 0.5% wt/vol gellan gum–loaded with $AuCl_3$) with increasing shear strain (left) and frequency (right).

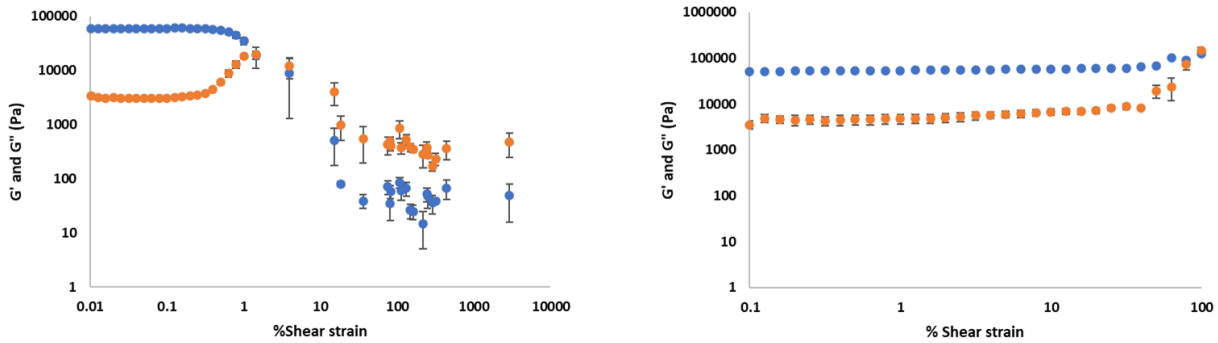

Figure S13. Elastic (G′, blue circles) and viscous (G′′, orange circles) moduli of DBS-CONHNH$_2$/gellan gum hydrogel (0.3% wt/vol DBS-CONHNH$_2$ and 1% wt/vol gellan gum) with increasing shear strain (left) and frequency (right).

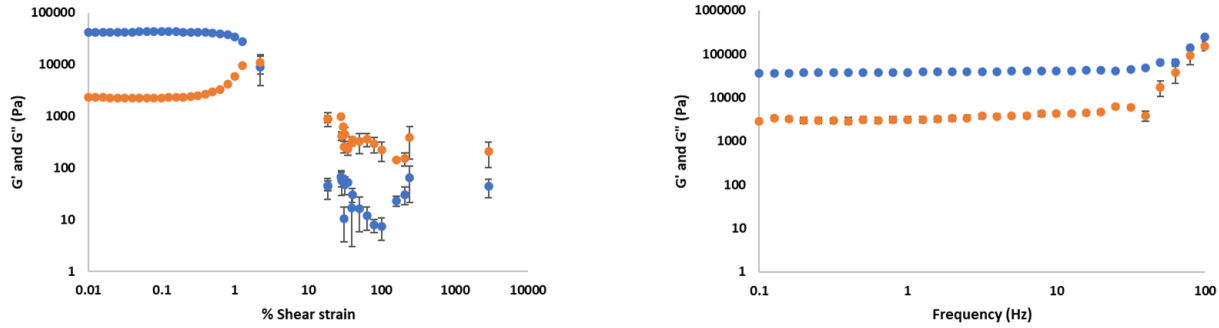

Figure S14. Elastic (G′, blue circles) and viscous (G′′, orange circles) moduli of DBS-CONHNH$_2$/gellan gum hydrogel (0.3% wt/vol DBS-CONHNH$_2$ and 1% wt/vol gellan gum –loaded with $AuCl_3$) with increasing shear strain (left) and frequency (right).

S5 AuNP patterning

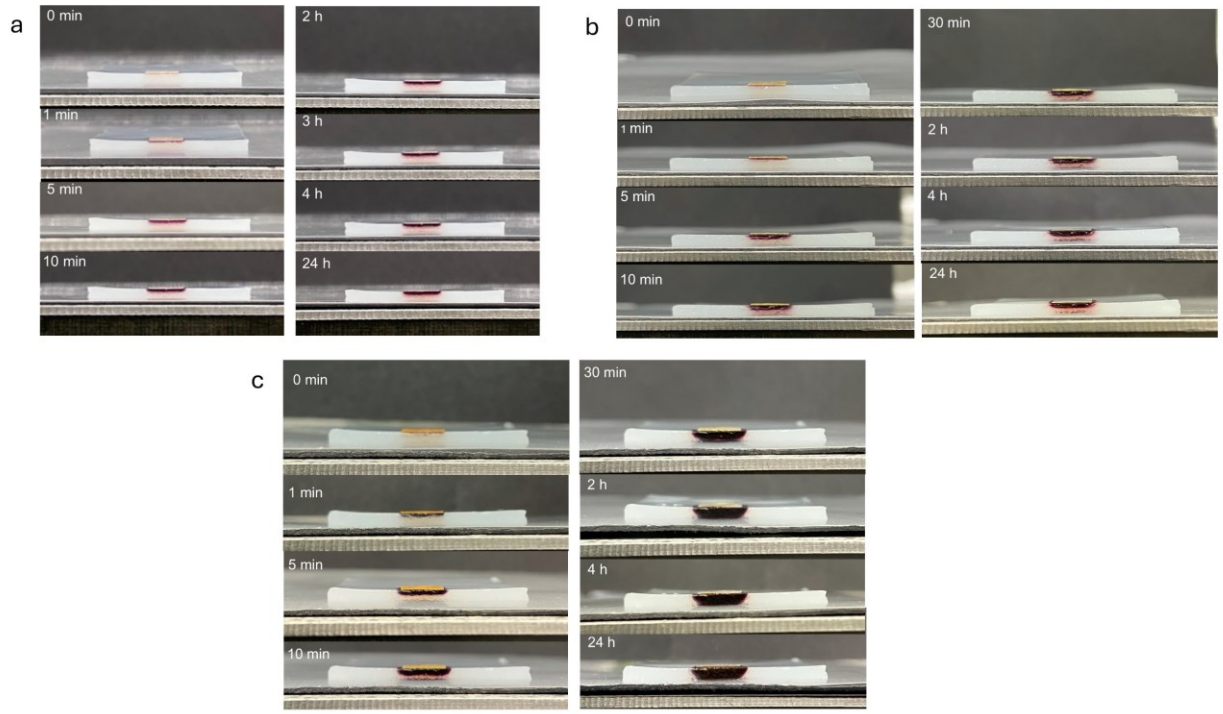

Figure S15. Photographs showing the side view of the $AuCl_3$ diffusion on DBS-$CONHNH_2$/gellan gum gel after a square filter paper soaked with $AuCl_3$ placed on top at concentrations of (a) 5 mM (b) 20 mM, and (c) 100 mM.

S5.1 Transmission Electron Microscopy (TEM)

AuNP-patterning gel samples were prepared as described in Section 4.2 of the paper. Materials from different regions were loaded onto HT-treated formvar/carbon coated grid. The samples were then negative stained with 2% aqueous uranyl acetate. The specimens were visualised using FEI Tecnai TF20 TEM operating at 120kV and images collected using FEI Ceta CCD camera.

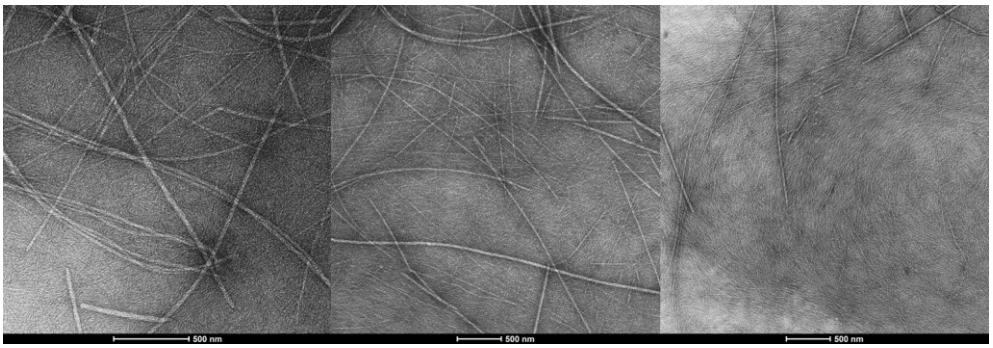

Figure S16. TEM images of non-patterned AuNPs regions on DBS-CONHNH$_2$/gellan gum gel. Scale bar of 500 nm.

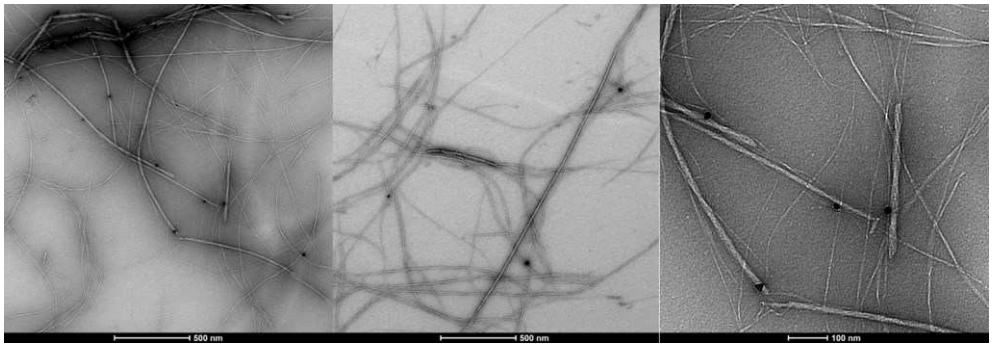

Figure S17. TEM images of patterned AuNP regions on DBS-CONHNH$_2$/gellan gum gel. Scale bar of 500 (left and middle) and 100 (right) nm.

S5.4 Scanning Electron Microscopy (SEM)

AuNP-patterned gel samples were prepared as described in Section 4.2 of the paper. Samples from regions patterned with/without AuNPs were frozen by immersion in slushy liquid nitrogen and then introduced into the cold stage of Polaron E5380 freeze-drier operating at -60 °C. Samples were freeze dried and then mounted onto SEM stubs. They were subsequently coated with 5 nm of gold palladium with the Polaron SC7640 sputter coater. Then visualized under the Jeol JSM 6490 LV SEM operating at 10 kV. Representative images were collected at 10-40k magnification.

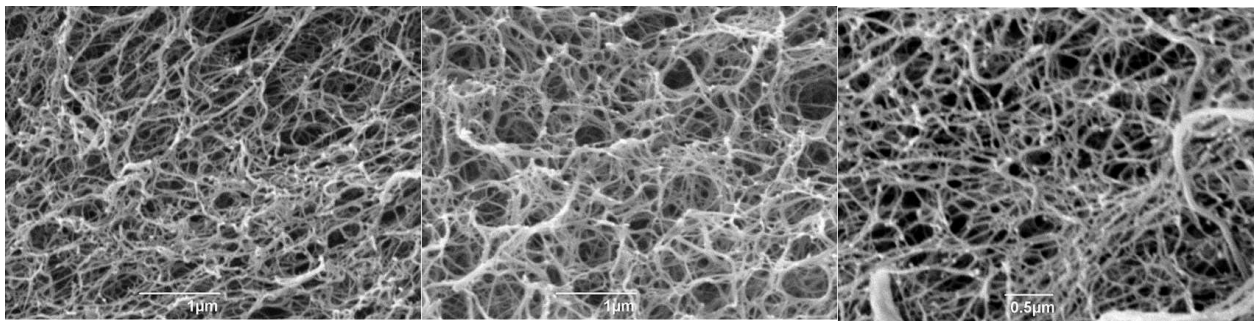

Figure S18. SEM images of non-patterned AuNP regions on DBS-CONHNH$_2$/gellan gum gel. Scale bar of 1 (left and middle) and 0.5 (right) µm.

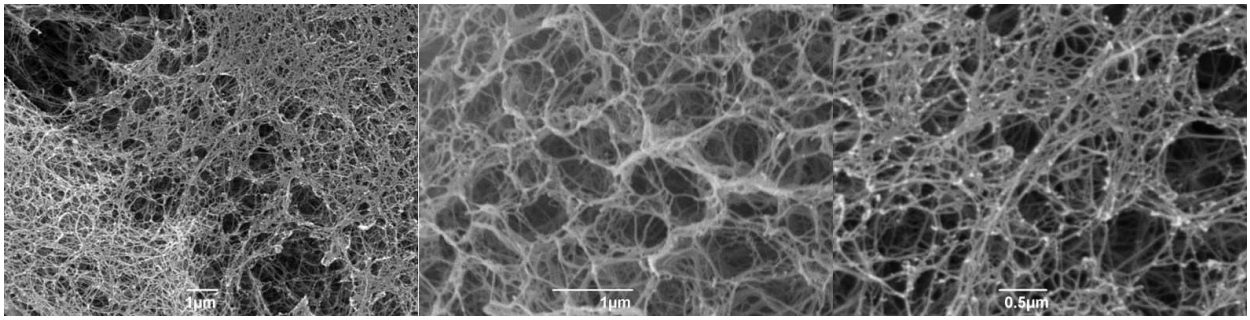

Figure S19. SEM images of patterned AuNP regions on DBS-$CONHNH_2$/gellan gum gel. Scale bar of 1 (left and middle) and 0.5 (right) µm.

S6 Biological Studies

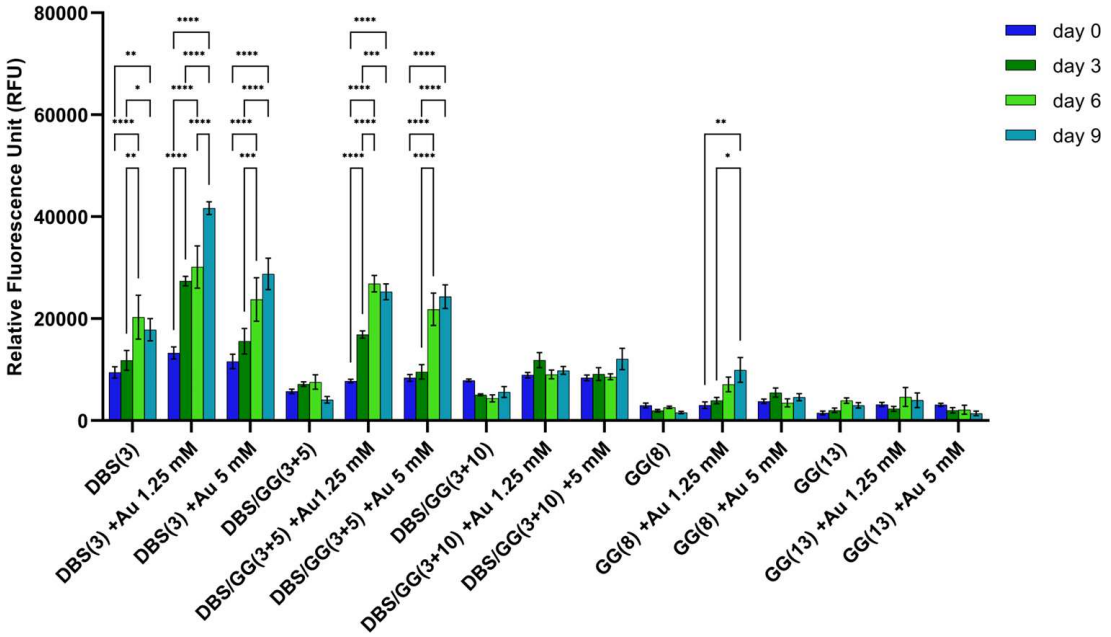

Figure S20. Metabolic activity of Y201 MSCs cultured onto the surface of DBS-$CONHNH_2$ (DBS), DBS-$CONHNH_2$/gellan gum (DBS+GG) and gellan gum (GG). Hydrogels were loaded with different $AuCl_3$ concentrations (1.25 mM or 5.0 mM). The number in brackets from left to right represents the concentration of DBS-$CONHNH_2$ and gellan gum in mg mL^{-1}, respectively. All gellan gum gels were crosslinked with $CaCl_2$. n=6, mean reported with error bars represent SEM: *$p < 0.05$, **$p < 0.01$, ***$p < 0.001$, ****$p < 0.0001$ (two-way ANOVA). Statistical analysis compares different conditions at the same time point (different to that in Figure 4).

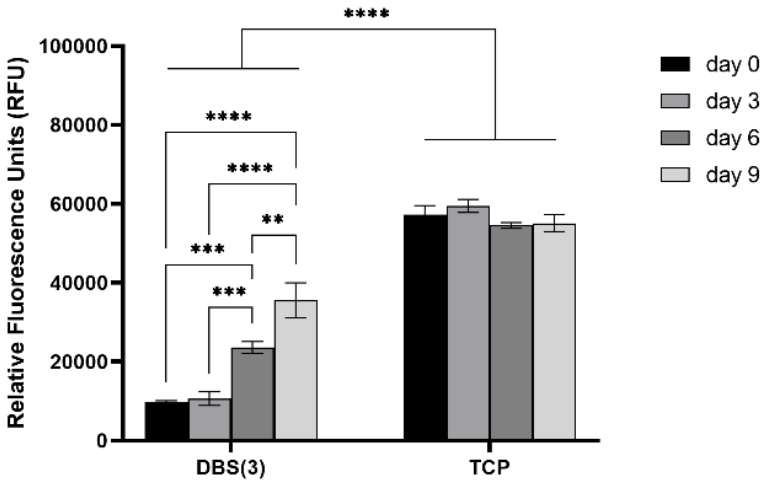

Figure S21. Metabolic activity of Y201 MSCs cultured onto the surface of DBS-$CONHNH_2$ (DBS, 3mg mL^{-1}) and tissue culture plastic (TCP). n=6, mean reported with error bars represent SEM: *p < 0.05, **p < 0.01, ***p < 0.001, ****p < 0.0001 (two-way ANOVA).

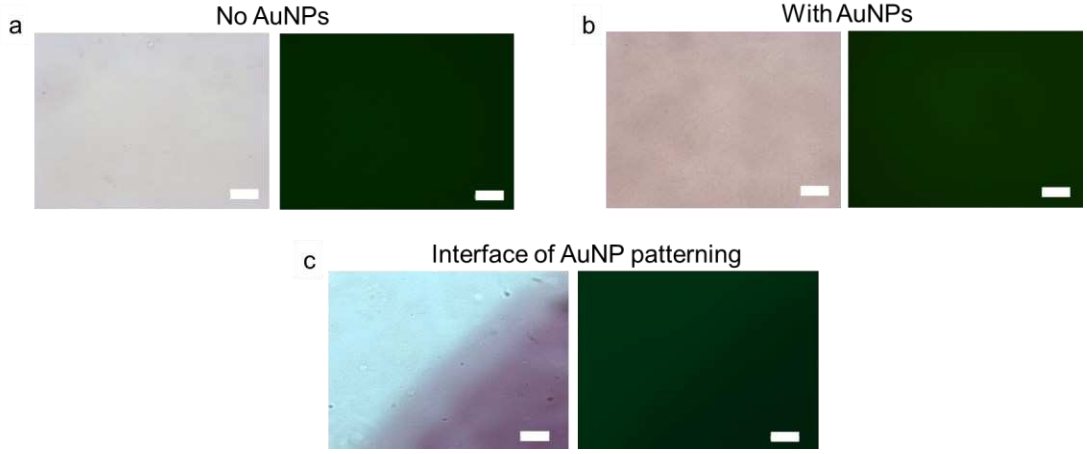

Figure S22. Bright field (left) and fluorescence (right) images of standard DBS-$CONHNH_2$/GG control hydrogel (a) without AuNPs, (b) with AuNPs. (c) Bright field (left) and fluorescence (right) of interface area from AuNP patterning on DBS-$CONHNH_2$/GG. These samples were stained with calcein AM as control. Scale bar 100 μm.

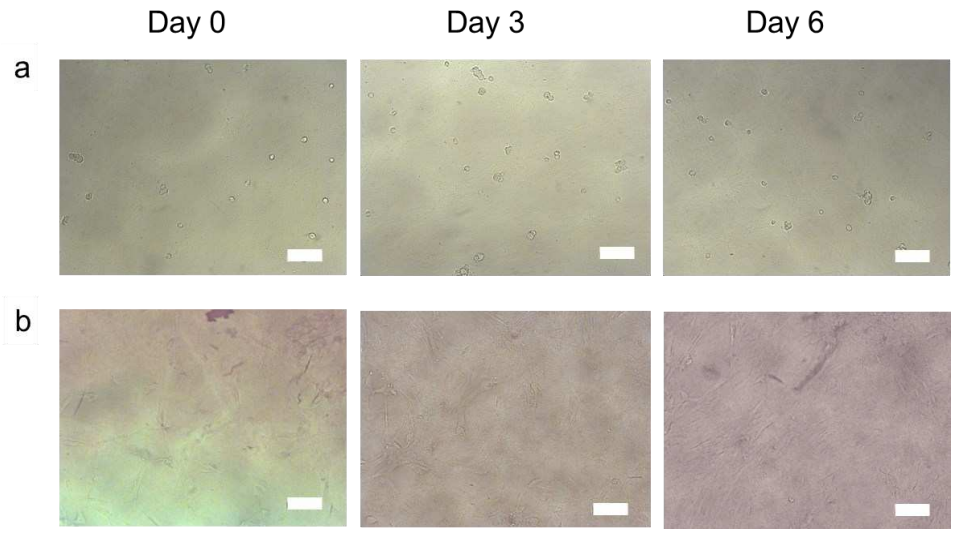

Figure S23. Bright field images of Y201 MSC growth on DBS-CONHNH$_2$/GG hydrogels (a) without AuNPs and (b) with AuNPs at day 0, 3 and 6. Scale bar of 100 μm.

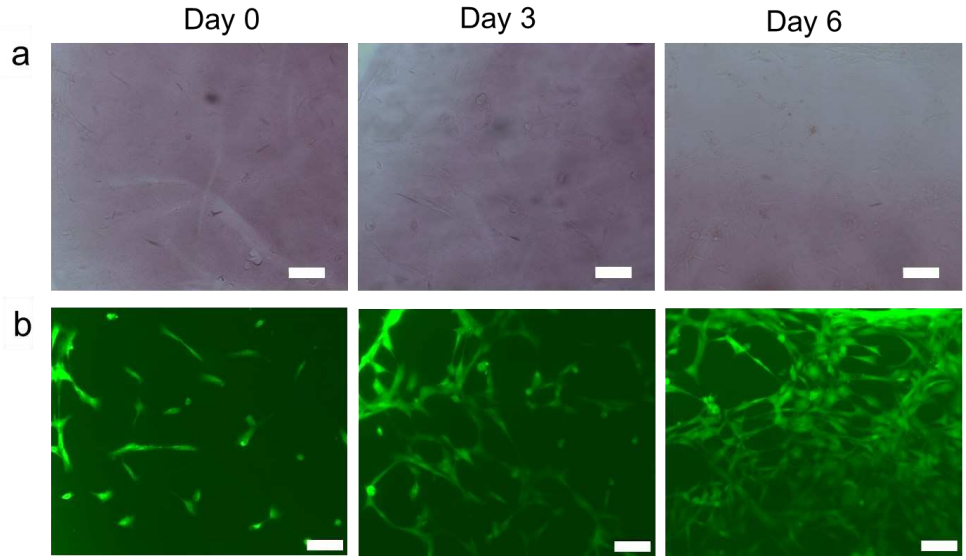

Figure S24. Bright field (top) and fluorescence (bottom) images of Y201 MSC growth on AuNP-loaded region of AuNPs star (5 mM) patterned DBS-CONHNH$_2$/GG hydrogel at day 0, 3 and 6 with Calcein AM staining. Scale bar of 100 μm.

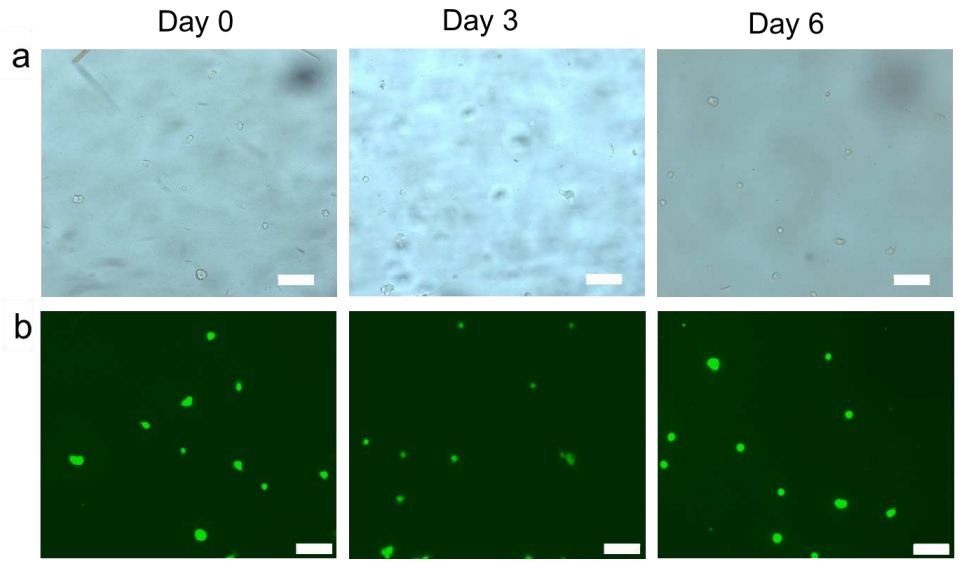

Figure S25. Bright field (top) and Fluorescence (bottom) images of Y201 MSC growth on AuNP-free region of AuNPs star (5 mM) patterned DBS-CONHNH$_2$/GG hydrogel at day 0, 3 and 6 with Calcein AM staining. Scale bar of 100 μm.

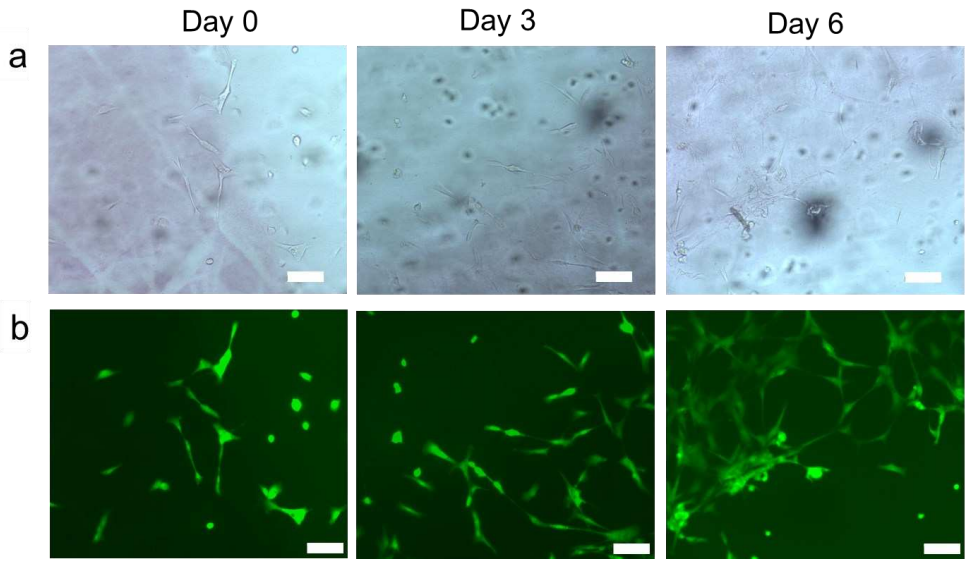

Figure S26. Bright field (top) and fluorescence (bottom) images of Y201 MSC growth on interface region of AuNP star (1.25 mM) patterned DBS-CONHNH$_2$/GG hydrogel at day 0, 3 and 6 with Calcein AM staining. Scale bar of 100 μm.

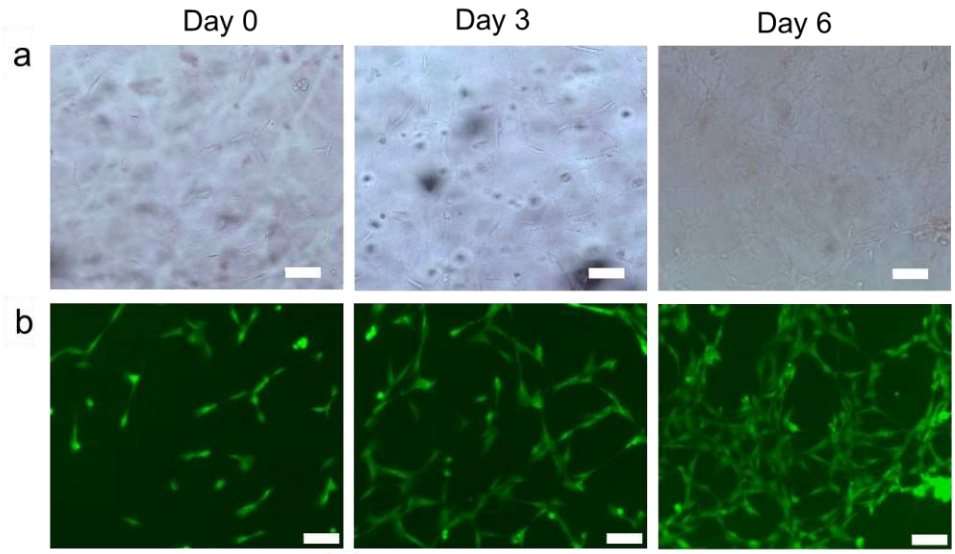

Figure S27. Bright field (top) and fluorescence (bottom) images of Y201 MSCs growth on AuNP region of AuNP star (1.25 mM) patterned DBS-CONHNH$_2$/GG hydrogel at day 0, 3 and 6 with Calcein AM staining. Scale bar of 100 μm.

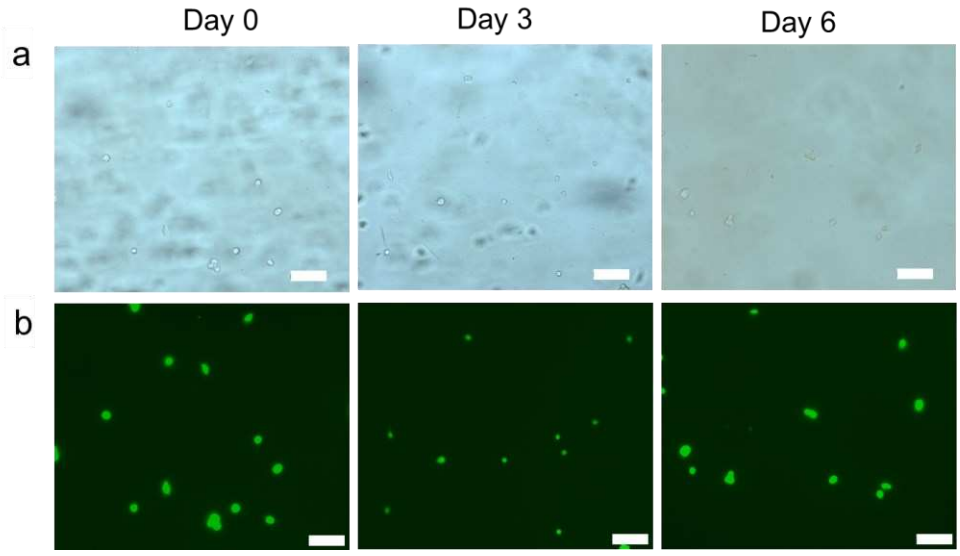

Figure S28. Bright field (top) and fluorescence (bottom) images of Y201 MSC growth on AuNP-free region of AuNPs star (1.25 mM) patterned DBS-CONHNH$_2$/GG hydrogel at day 0, 3 and 6 with Calcein AM staining. Scale bar of 100 μm.

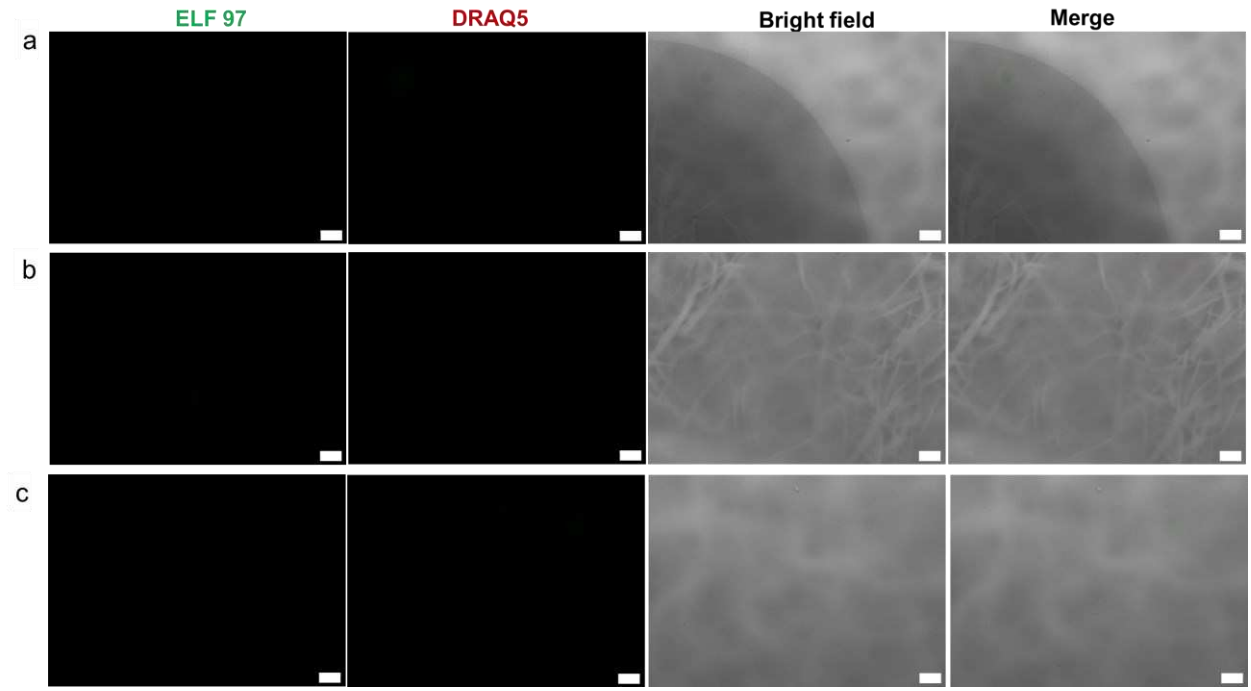

Figure S29. Fluorescence images of DBS-$CONHNH_2$/GG control hydrogel (a) interface, (b) with AuNPs and (c) without AuNPs area from AuNP patterning on DBS-$CONHNH_2$/GG. These samples were stained with ELF 97 and DRAQ5 as control. Scale bar of 100 μm.

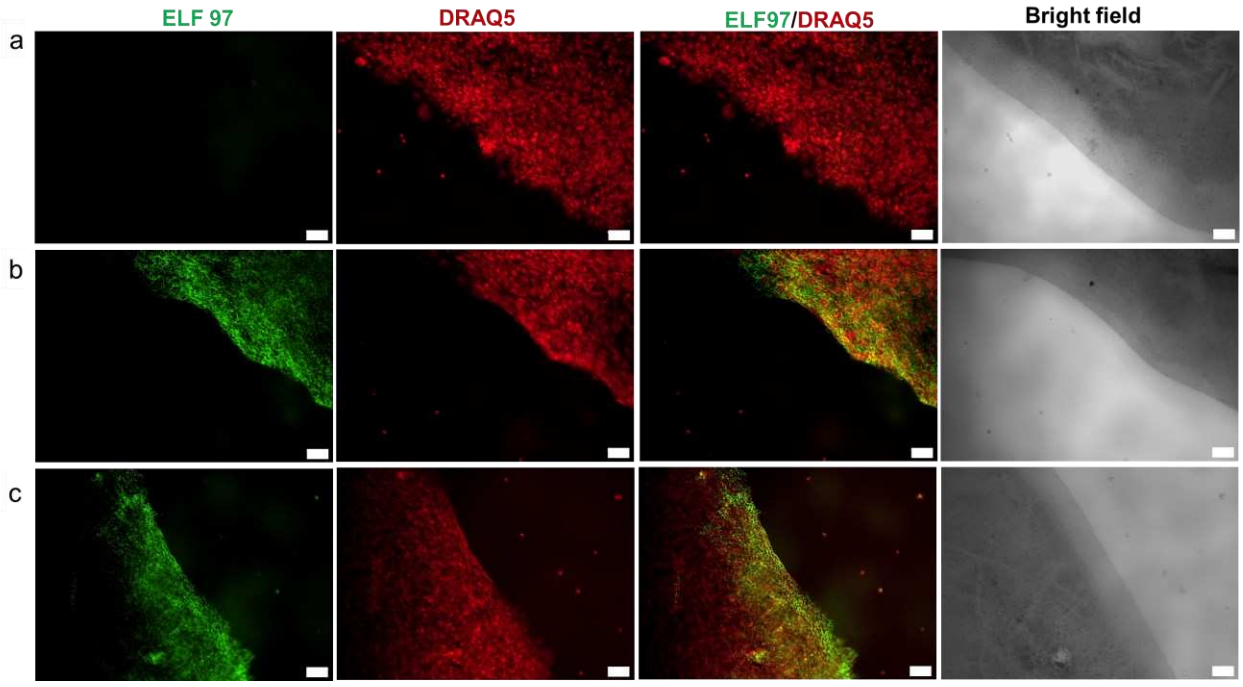

Figure S30. Fluorescence images of Y201 MSC differentiation on interface of AuNP patterning on DBS-$CONHNH_2$/GG at (a) day 7, (b) day 14 and (c) day 21. These samples were stained with ELF 97 and DRAQ5. Scale bar of 100 μm.

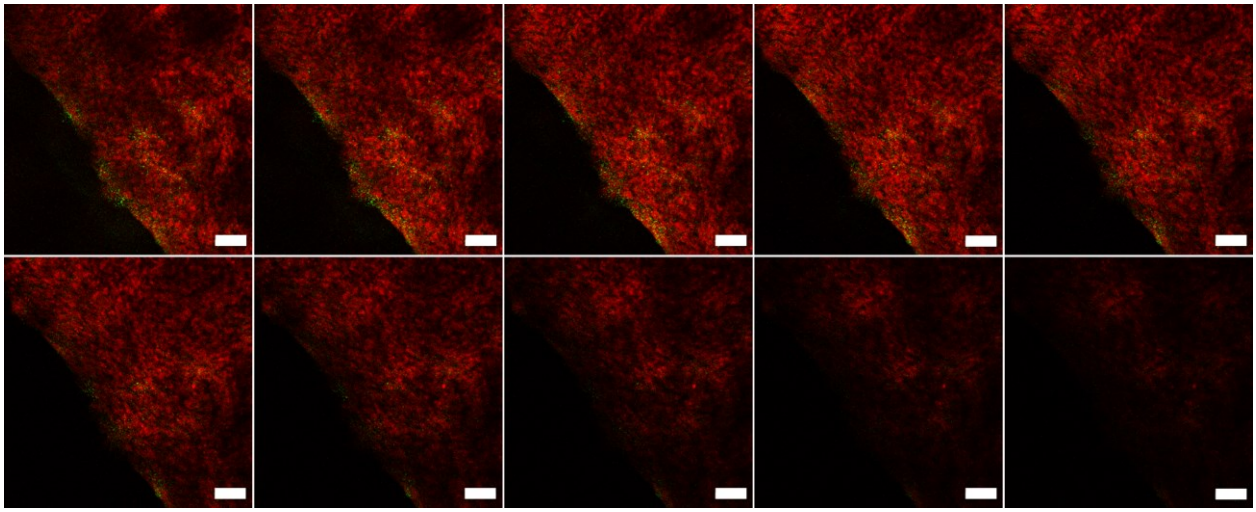

Figure S31. Z-stack using confocal microscope of Y201 MSC differentiation on interface of AuNP patterning on DBS-$CONHNH_2$/GG at day 21. These samples were stained with ELF 97 and DRAQ5. Scale bar of 100 μm.

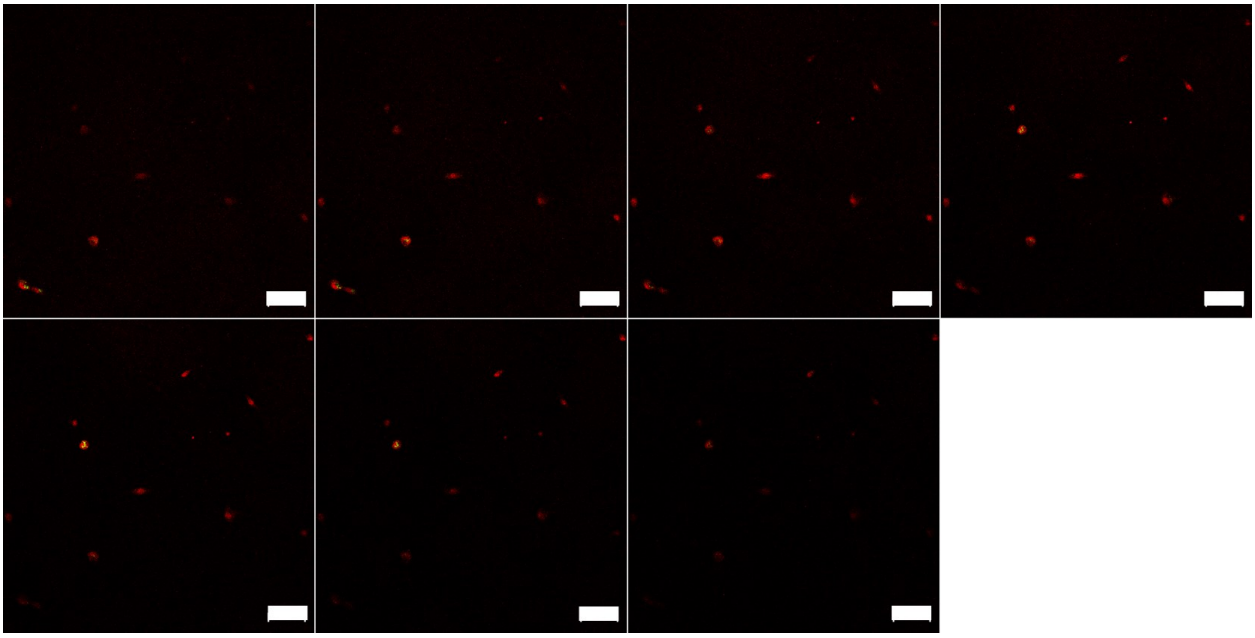

Figure S32. Z-stack using confocal microscope of Y201 MSC differentiation on NO AuNP region of AuNP patterning on DBS-$CONHNH_2$/GG at day 21. These samples were stained with ELF 97 and DRAQ5. Scale bar of 100 μm.

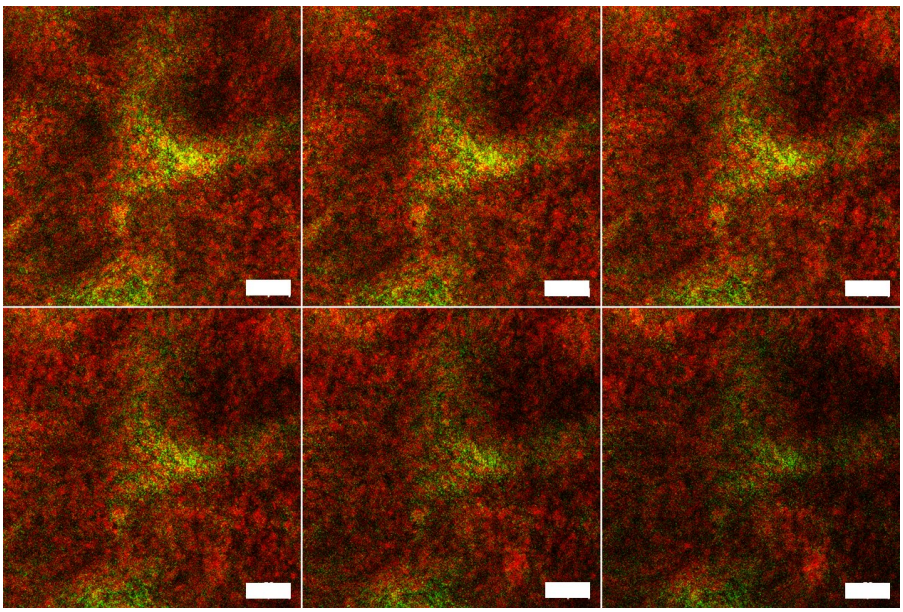

Figure S33. Z-stack using confocal microscope of Y201 MSC differentiation on AuNP region of AuNP patterning on DBS-$CONHNH_2$/GG at day 21. These samples were stained with ELF 97 and DRAQ5. Scale bar of 100 μm.

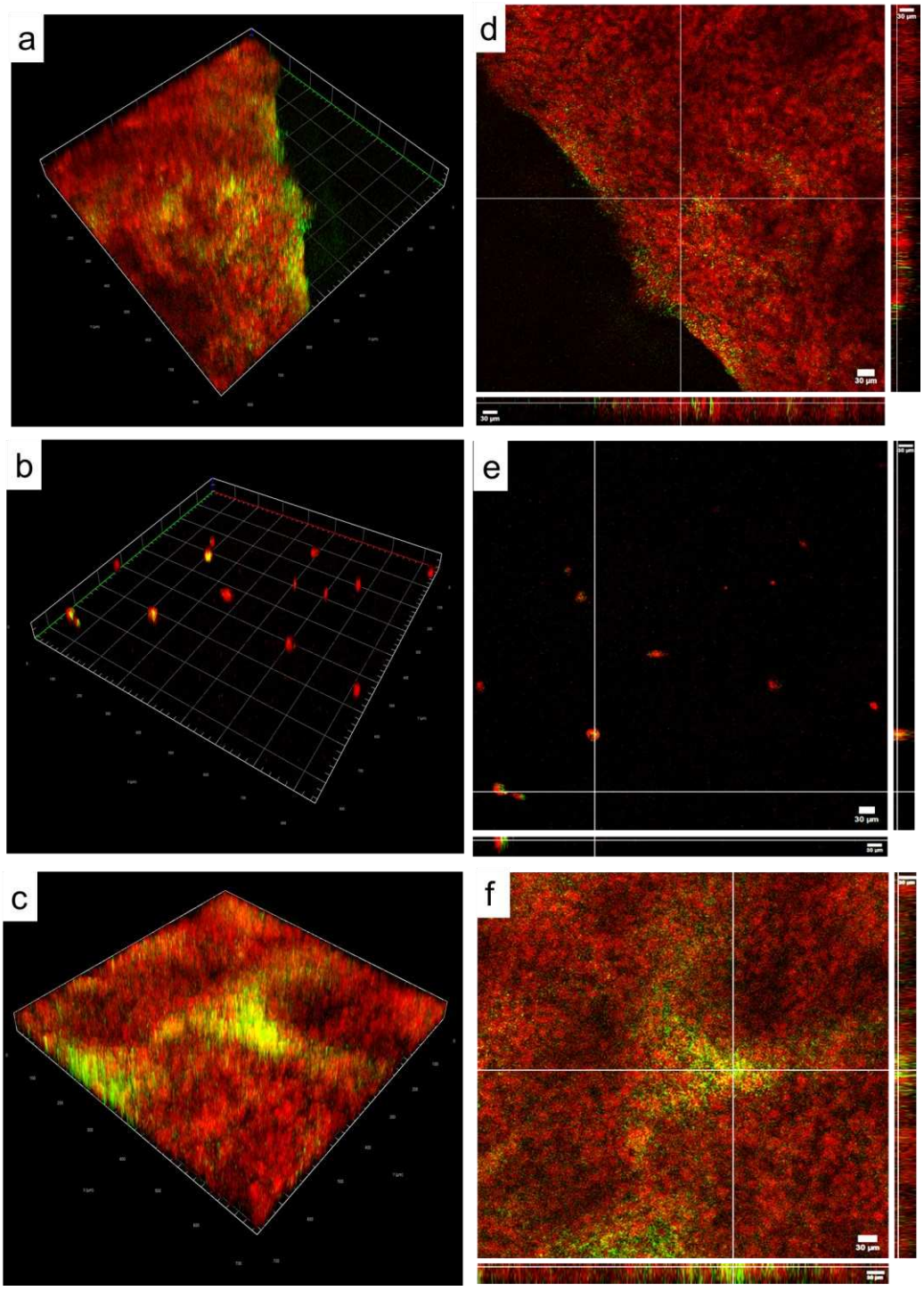

Figure S34. 3D (left) and orthogonal view (right) images from confocal laser scanning microscopy of Y201 MSC differentiation on AuNP patterned scaffold stained with ELF 97 (ALP staining showing yellow-green spots) and DRAQ5 (nuclear staining showing red) on day 21. (a,d) Interface, (b,e) no AuNP and (c,f) on AuNP patterning scaffold. Scale bar of 30 µm.